

HIGH WIND AND BREAKING WAVE MEASUREMENTS WITH SAR DEPOLARIZED RETURNS

Paul A. Hwang

Remote Sensing Division, Naval Research Laboratory, Washington DC, USA

Email: paul.hwang@nrl.navy.mil

ABSTRACT

The wind generates a distribution of small slope waves and sporadic steep breaking events. Such double structure of the sea surface is expected to have a strong impact on the radar scattering from the ocean surface. The signature of the double structure is in the wind speed dependence of radar returns: linear for scattering from gentle waves and cubic for breaking contribution. The composite-surface Bragg resonance (CB) theory describes the former very well. Detection of the breaking contribution remains difficult. Here we show that the depolarized (de-pol, or cross-polarized) radar return exhibits the typical double structure, its wind speed dependence increases from linear in low to moderate wind speeds to cubic in high winds. The increased sensitivity of the de-pol returns in high winds is ideal for hurricane wind retrieval. The strong breaking connection offers an opportunity to measure wave breaking and the associated energy dissipation and area of foam coverage from space, their quantification is important for air-sea interaction study and electromagnetic and electro-optical remote sensing.

Index Terms— *Depolarized radar cross section, Breaking wave, Hurricane wind*

1. INTRODUCTION

Active radar backscatters and passive microwave emissions from the ocean surface are our major sources of wind measurements in the ocean. Without spaceborne active and passive microwave sensors, weather observations in three quarters of the earth surface would have to rely on the limited number of instrumented buoys and weather ships distributed irregularly over the ocean. Clearly, active and passive microwave remote sensing has become an integral part of our weather monitoring systems.

Phillips (1988) addresses the radar scattering problem considering the structure of ocean surface waves, which are the roughness elements that scatter the radar waves on the ocean surface. He establishes an analytical framework of the double structure of sea surface scatterers. Applying the results of his detailed wave dynamic analysis (Phillips, 1985) and radar scattering theories (e.g., Valenzuela, 1978), he shows that the wind speed dependence of the normalized radar cross section (NRCS) is expected to be linear in the Bragg contribution and cubic in the breaking contribution. However, based on subsequent comparisons of the theory with several field observations, he concludes that the assembled data do not reveal the cubic wind speed dependence expected of the breaking contribution. The data set he examined in most detail (Guinard et al., 1971) reveals a comprehensive linear dependence of NRCS on wind speed throughout the whole range of radar frequencies and incidence angles in the data set (0.428 to 8.91 GHz and 30° to 85°, respectively).

Interestingly, recent analysis of the polarimetric radar returns shows a distinctive double structure in the de-pol radar backscatter (Hwang et al., 2010a, b). In Section 2, I present an excerpt of the results from analyzing the co-pol (σ_{VV} and σ_{HH} , respectively, vertical transmit vertical receive and horizontal transmit horizontal receive) and de-pol (σ_{VH} , horizontal transmit vertical receive or vertical transmit horizontal receive) returns from RADARSAT-2 (R2). The co-pol data are in general agreement with the CB theory but de-pol data show significant departure from theoretical prediction in high winds. Of special interest is the wind speed dependence of the de-pol return -- linear in mild to moderate winds and cubic in high winds -- reflecting the characteristics of the double structure described by Phillips (1988). The significant connection between de-pol returns with breaking offers an opportunity to monitor wind wave breaking from space, and the enhanced sensitivity in high winds is especially valuable for retrieval of high wind speeds in hurricanes or typhoons (Section 3).

Presently, wind retrieval uses co-pol microwave returns. available theoretical and experimental evidence suggests that saturation or dampening of co-pol radar backscatter occurs across a wide range of radar frequencies and wind speeds [e.g., Donnelly et al., 1999; Yueh et al., 2001; Donelan et al., 2004; Fernandez et al., 2006; Shen et al., 2009]. The issues of accuracy and feasibility of high wind speed using co-pol NRCS remain unsettled. The ability to retrieval high wind using de-pol microwave

returns is especially valuable for securing our ability to measure high wind speeds from space. A summary is given in Section 4.

2. ANALYSIS OF RADARSAT-2 RETURNS

Quad-polarization (quad-pol) and dual-polarization (dual-pol) measurements with de-pol radar returns from the ocean surface are now available from many satellites, among them the R2. Hwang et al. (2010a, b) present analysis results of quad-pol (414 points) and dual-pol (372 points) backscatter data and collocated wind velocities from ocean buoys maintained by the National Data Buoy Center (NDBC). Figure 1 displays examples of the radar returns of quad-pol data set as a function of wind speed, U_{10} . The curves predicted by the CB theory (Valenzuela, 1978) and the empirical geophysical model function (GMF) CMOD5 (Hersbach et al., 2007; Mouche et al., 2005) are also shown for comparison. The input surface roughness spectrum for the CB computation is the parameterization function of short scale wave spectra collected from the ocean (Hwang, 2008) combined with the directional distribution function developed by Donelan et al. (1985) with subsequent modifications (Donelan and Pierson, 1987; Banner, 1990; Plant, 2002).

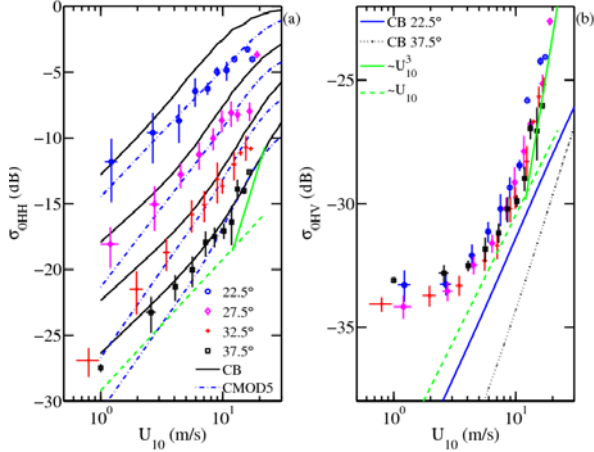


Figure 1. Comparison of R2 measured NRCS, theoretical prediction, and empirical GMF. (a) Quad-pol σ_{0HH} , and (b) quad-pol σ_{0VH} . Symbols: R2 measurements averaged in four ranges of incidence angle, θ (the short line segment on the symbol represents one standard deviation of data scatter); solid curves: CB theory, dashed-and-dotted curves: CMOD5 (co-pol only), both theory and GMF are computed for $\theta=22.5^\circ, 27.5^\circ, 32.5^\circ$ and 37.5° . The light-green dashed and solid curves show, respectively, the linear and cubic wind speed dependence.

The agreement between R2 co-pol data, CB theory and GMF is generally within a couple of dB. The difference between σ_{0VH} and the CB theory is somewhat larger especially at both ends of the wind speed range and will be further discussed in the next paragraph. In contrast to the

co-pol returns, there are two notable features in the de-pol data: (1) the incidence angle dependence is considerably weaker, and (2) the transition of wind speed dependence from linear in low and moderate winds to cubic in high winds is much more distinctive. These observations suggest that for the co-pol returns the breaking contribution is relatively small in comparison to the Bragg contribution. For de-pol, the Bragg return is zero without tilting so breaking contributions stand out. Further quantification of the result, however, requires a reliable model of the breaking contributions of radar co-pol and de-pol returns.

Figure 2(a) plots together quad-pol and dual-pol σ_{0VH} . There is good agreement between the two data sets in high winds. A difference of about 5 to 6 dB in low winds reveals the much larger dual-pol noise floor. The quad-pol product is known to have extremely low noise floor and the channel cross-talk has been corrected. Assuming that the system noise is -30 dB for dual-pol and -36 dB for quad-pol, the data are averaged in two θ bins ($25\pm5^\circ$ and $35\pm5^\circ$) with noise subtracted. The results are compared with the CB theory in Figure 2(b). The agreement of de-pol data with the CB theory is reasonably good in mild and moderate winds ($U_{10} < \sim 10$ m/s). Because R2 measurements include both Bragg and breaking contributions and the CB theory only accounts for the former, the difference between the R2 data and CB theory is an estimate of the wave breaking contribution, σ_{0VHb} .

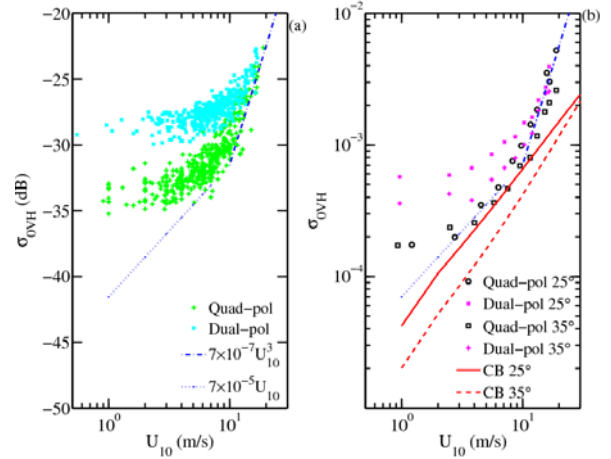


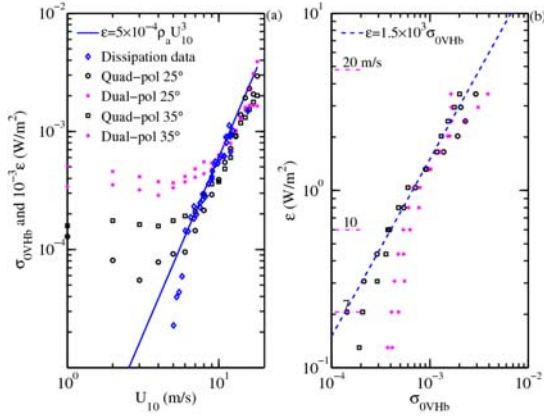
Figure 2. Comparison of de-pol returns from quad-pol and dual-pol data sets. (a) Effect of system noise on the appearance of wind speed dependence, and (b) comparison of average σ_{0VH} with the CB theory. The assumed system noise (-30 dB for dual-pol and -36 dB for quad-pol) is removed in (b). The transition of linear to cubic wind speed dependence of σ_{0VH} is illustrated with dotted and dotted-and-dashed curves, respectively.

3. WAVE BREAKING MEASUREMENT AND WIND SPEED RETRIEVAL

a. Wave breaking analysis

Surface wave breaking is one of the most important sources of turbulence and energy dissipation in the upper ocean. Theoretical and experimental analyses lead to a cubic dependence of the energy dissipation rate, ε , on wind speed, U_{10} (Phillips, 1985; Felizardo and Melville, 1995; Terray et al., 1996; Hanson and Phillips, 1999; Gemmrich and Farmer, 2004; Hwang and Sletten, 2008; Hwang, 2009). Figure 3a compares the estimates of ε from several field experiments (Felizardo and Melville, 1995; Terray et al., 1996; Gemmrich and Farmer, 2004) and the breaking contribution of de-pol return, σ_{0VHb} . The cubic wind speed dependence of both ε and σ_{0VHb} is easily detectable (the trend in radar data at low wind speeds is corrupted by the low signal-to-noise ratio). The energy dissipation rate per unit area of the ocean surface (in W/m^2) can be approximated by $\varepsilon = 5 \times 10^{-4} \rho_a U_{10}^3$ (Hwang and Sletten, 2008; Hwang, 2009), where ρ_a is air density ($\sim 1.2 \text{ kg/m}^3$). Conceivably, we can measure ocean surface energy dissipation rate from space using the de-pol radar return, an empirical relation of $\varepsilon = 1.5 \times 10^3 \sigma_{0VHb}$ is established (Figure 3b). Quad-pol product with its low noise floor is especially suitable for measuring wave breaking and energy dissipation from space.

Figure 3. (a) Comparison of energy dissipation rate and the



breaking contribution of de-pol radar return as a function of wind speed. (b) Feasibility of measuring ocean surface energy dissipation rate from space using de-pol radar returns.

b. Wind speed inversion

The inversion of wind speed from NRCS measurements is typically done through the look up table (LUT). For example, at the European Space Agency (ESA), the NRCS is precalculated with the GMF (e.g., CMOD5) for wind speeds from 1 to 60 m/s in 0.5 m/s bins, incidence angles from 15 to 69 degrees in 1 degree bins, and relative wind directions in 5 degree bins. The backscatter is linearly interpolated to the correct incidence angle but no

interpolation is done for wind speed and wind direction, so the resolution of the ESA wind product is 0.5 m/s in wind speed and 5 degrees in wind direction (Hersbach, 2003).

The available R2 data set is not large enough for the purpose of producing a de-pol GMF. However, the dependence of de-pol return on incidence angle and wind direction is relatively weak. We can use the following empirical equation for wind speed inversion from the de-pol return,

$$U_{10} = \begin{cases} 5.1178q^2 + 1.6664q + 54.235, & \theta \leq 30^\circ \\ -2.6444q^2 - 1.3433q + 33.106, & \theta > 30^\circ \end{cases} \quad (1)$$

where q is the de-pol return in dB, $q = \sigma_{0HV}^{dB}$. Figure 4 compares the wind speed inversion using de-pol return via (1) and co-pol return through CMOD5 LUT. The CMOD5 GMF is for σ_{0VV} only. The polarization ratio proposed by Mouche et al. (2005) and the empirical modification presented in the Appendix of Hwang et al. (2010b) are used to generate two sets of σ_{0HH} LUT (with M05 and R2 appended when distinction is needed). The statistics of bias (B), proportionality constant or slope of fitting (s), rms difference (D), correlation coefficient or normalized cross covariance (R), and scatter index (I) are listed in Table 1. The overall improvement of wind speed retrieval using the de-pol radar return in comparison to those derived from the co-pol returns is evident. Further improvement in performance of de-pol wind retrieval can be expected when larger data sets become available to make use of more refined incidence angle and azimuth angle dependence.

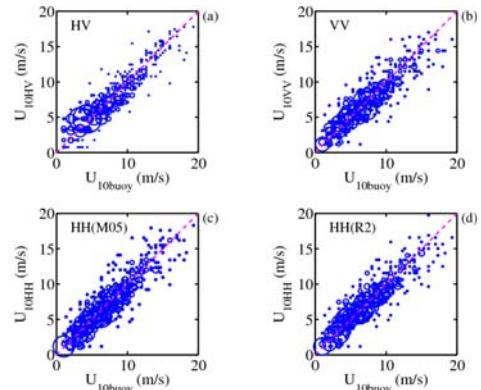


Figure 4. Wind speed inversion using: (a) σ_{0VH} , (b) σ_{0VV} , (c) σ_{0HH} with polarization ratio of Mouche et al. (2005), and (d) σ_{0HH} with the modification of the polarization ratio described in the Appendix of Hwang et al. (2010b).

Table 1. Regression statistics of wind speeds measured by buoy and derived with de-pol and co-pol NRCS. (B : bias, s : proportionality constant or slope of fitting, D : RMS difference, R :

correlation coefficient or normalized cross covariance, and I : scatter index.)

All data (427 points)					
	B	s	D	R	I
HV	0.000	0.983	1.498	0.916	0.207
VV	-0.139	0.968	1.654	0.897	0.228
HH M05	-0.114	0.988	1.668	0.901	0.230
HH R2	-0.079	0.977	1.624	0.901	0.224
U > 5 m/s (268 points)					
	B	s	D	R	I
HV	-0.375	0.963	1.447	0.897	0.155
VV	-0.412	0.954	1.774	0.837	0.191
HH M05	-0.265	0.980	1.794	0.845	0.187
HH R2	-0.320	0.963	1.721	0.843	0.187

c. Wave breaking analysis without radar scatter computation

In the absence of radar backscattering computation, we can still make use of the observed quasi-linear wind speed dependence of the de-pol return based on the CB computation (Figure 2b) to devise a simple method for dissipation estimation using the de-pol data. Figure 5 shows the wind speed dependence of the raw σ_{0VH} data (prior to bin average) with the assumed -36 dB noise subtracted.

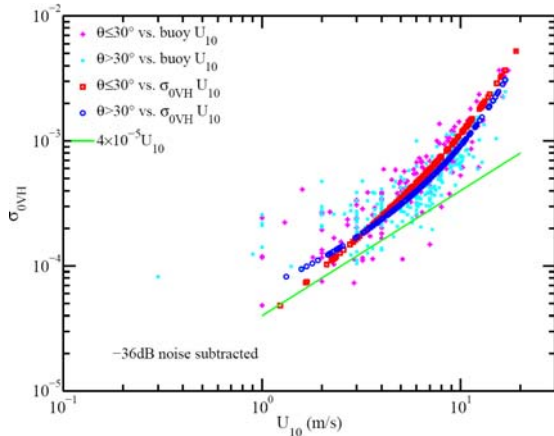


Figure 5. Wind speed dependence of the de-pol radar return (with assumed -36 dB noise subtracted). The dependence is shown with both sets of wind speeds measured by buoy and inverted using σ_{0VH} (1). The linear wind dependence curve near the lower bound of data cloud can be used as an approximation of non-breaking contribution in the absence of radar scattering computation.

The de-pol returns are plotted against both sets of wind speeds measured by buoy and inverted from de-pol return using (11). The curve with linear wind dependence

depicted in the figure ($4 \times 10^{-5} U_{10}$) form an approximate lower bound of the data cloud. Using this lower bound as an estimation of the non-breaking contribution, an approximation of the breaking contribution of de-pol return, σ_{0VHb}^a , can be written as

$$\sigma_{0VHb}^a = \max(0, \sigma_{0VH} - 4 \times 10^{-5} U_{10}). \quad (2)$$

Figure 6(a) shows the comparison of ε , σ_{0VHb} , and two sets of σ_{0VHb}^a (with buoy U_{10} and de-pol inverted U_{10} in (2)), all four quantities display the cubic wind speed dependence typical of surface wave breaking. The dissipation rate data are assembled from several field experiments as described earlier. The result of approximation using wind speeds inverted from σ_{0VH} is of special interest because it does not rely on external source for the purpose of breaking detection from space. A slightly modified relationship between the dissipation rate and the de-pol radar return without the benefit of radar scattering computation can be expressed as (Figure 6b)

$$\varepsilon = 1.0 \times 10^3 \sigma_{0VHb}^a, \quad (3)$$

where σ_{0VHb}^a is computed with (2), and U_{10} in (2) computed with (1).

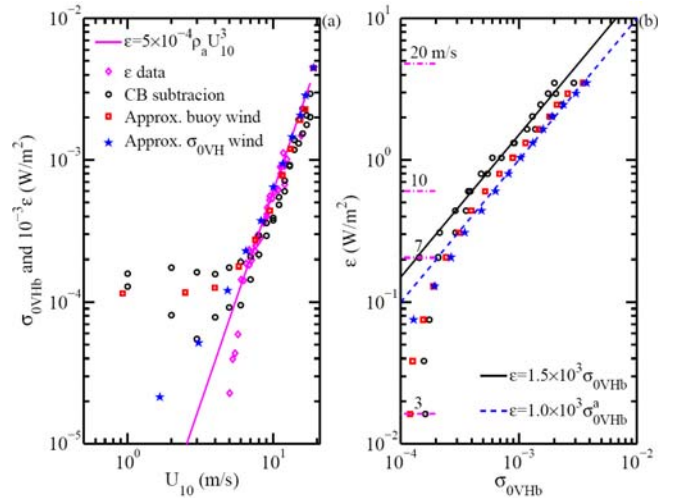


Figure 6. (a) Comparison of energy dissipation rate and the breaking contribution of de-pol radar return as a function of wind speed. Results of the latter quantities using wind speed derived from de-poly return and measured by buoy are shown. (b) Feasibility of measuring ocean surface energy dissipation rate from space using de-pol radar returns without external sources of input.

4. SUMMERY

The de-pol radar backscatter measurements from the ocean surface are now routinely available from many

satellites carrying polarimetric radars. In this paper, co-pol and de-pol backscatter from R2 quad-pol product collocated with NDBC buoys are assembled to investigate the wind speed dependence. The most significant result of this investigation is that the de-pol radar return from the ocean surface does not saturate in high winds. Furthermore, the wind speed dependence of de-pol return increases from linear in moderate and low winds to cubic in high winds, reflecting the double structure of the ocean surface roughness relevant to microwave remote sensing of the ocean. This is in a drastic contrast to the co-pol returns, of which an incidence-and-azimuth-angle-dependent saturation or dampening trend develops in high winds and the sensitivity of co-pol returns to wind speed decreases toward high winds. As a result, the wind speed retrieved with de-pol backscatter is more accurate than those retrieved with co-pol data in hazardous storm conditions such as hurricanes and typhoons. Wind speed inversion using the de-pol radar return, even with very coarse incidence angle sorting and without making use of azimuthal dependence, performs much better than co-pol wind retrieval, which requires the azimuthal information (Figure 4 and Table 1). The nearly cubic wind speed dependence of the depolarized radar backscatters in high wind speeds reflects significant breaking wave contributions and offered the opportunity to make breaking wave measurements from space (Figure 6).

5. REFERENCES

- Banner, M. L. (1990), Equilibrium spectra of wind waves, *J. Physic. Oceanogr.*, *20*, 966-984.
- Donelan, M. A., J. Hamilton, and W. H. Hui (1985), Directional spectra of wind-generated waves, *Phil. Trans. Royal Soc. Lond.*, *A315*, 509-562.
- Donelan, M. A., B. K. Haus, N. Reul, W. J. Plant, M. Stiassnie, H. C. Graber, O. B. Brown, and E. S. Saltzman (2004), On the limiting aerodynamic roughness of the ocean in very strong winds, *Geophys. Res. Lett.*, *31*, L18306, doi: 10.1029/2004GL019460.
- Donelan, M. A., and W. J. Pierson (1987), Radar scattering and equilibrium ranges in wind-generated waves with application to scatterometry, *J. Geophys. Res.*, *92*, 4971-5029.
- Donnelly, W. J., J. R. Carswell, and R. E. McIntosh (1999), Revised ocean backscatter models at C and Ku band under high-wind conditions, *J. Geophys. Res.*, *104*, 11485-11497.
- Felizardo, F., and W. K. Melville (1995), Correlations between ambient noise and the ocean surface wave field, *J. Phys. Oceanogr.*, *25*, 513-532.
- Fernandez, D. E., J. R. Carswell, S. Frasier, P. S. Chang, P. G. Black, and F. D. Marks (2006), Dual-polarized C- and Ku-band ocean backscatter response to hurricane-force winds, *J. Geophys. Res.*, *111*, C08013, doi: 10.1029/2005JC003048.
- Gemmrich, J. R., and D. M. Farmer (2004), Near-surface turbulence in the presence of breaking waves, *J. Phys. Oceanogr.*, *34*, 1067-1086.
- Guinard, N. W., J. T. Ransone, and J. C. Daley, (1971), Variation of the NRCS of the sea with increasing roughness. *J. Geophys. Res.*, *76*, 1525-1538.
- Hanson, J. L., and O. M. Philips (1999), Wind sea growth and dissipation in the open ocean, *J. Phys. Oceanogr.*, *29*, 1633-1648.
- Hersbach, H. (2003), CMOD5 – An improved geophysical model function for ERS C-band scatterometry, *ECMWF Tech. Memo. No. 395*, 52 pp., European Centre for Medium-Range Weather Forecasts, Reading, England.
- Hersbach, H., A. Stoffelen, and S. de Haan (2007), An improved C-band scatterometer ocean geophysical model function: CMOD5, *J. Geophys. Res.*, *112*, C03006, doi:10.1029/2006JC003743.
- Hwang, P. A. (2008), Observations of swell influence on ocean surface roughness, *J. Geophys. Res.*, *113*, C12024, doi:10.1029/2008JC005075.
- Hwang, P. A. (2009), Estimating the effective energy transfer velocity at air-sea interface, *J. Geophys. Res.*, *114*, C11011, doi:10.1029/2009JC005497.
- Hwang, P. A., and M. A. Sletten (2008), Energy dissipation of wind-generated waves and whitecap coverage, *J. Geophys. Res.*, *113*, C02012, doi:10.1029/2007JC004277.
- Hwang, P. A., B. Zhang, and W. Perrie, 2010a: Depolarized radar return for breaking wave measurement and hurricane wind retrieval. *Geophys. Res. Lett.*, *37*, L01604, doi:10.1029/2009GL041780.
- Hwang, P. A., B. Zhang, J. V. Toporkov, and W. Perrie, 2010b: Comparison of composite Bragg theory and quad-polarization radar backscatter from RADARSAT-2: With applications to wave breaking and high wind retrieval. *J. Geophys. Res.*, doi:10.1029/2009JC005995 (in press).
- Mouche, A. A., D. Hauser, J. Daloze, and C. Guerin (2005), Dual-polarization measurements at C-band over the ocean: Results from airborne radar observations and comparison with ENVISAT ASAR data, *Trans. Geos. Rem. Sens.*, *43*, 753-769.
- Phillips, O. M. (1985), Spectral and statistical properties of the equilibrium range in wind-generated gravity waves, *J. Fluid Mech.*, *156*, 505-531.
- Phillips, O. M. (1988), Radar returns from the sea surface – Bragg scattering and breaking waves, *J. Phys. Oceanogr.*, *18*, 1065-1074.
- Plant, W. J. (2002), A stochastic, multiscale model of microwave backscatter from the ocean, *J. Geophys. Res.*, *107*, C93120, doi:10.1029/2001JC000909.
- Shen, H., Y. He, and W. Perrie (2009), Speed ambiguity in hurricane wind retrieval from SAR imagery, *Int. J. Rem. Sens.*, *30*, 2827 – 2836.
- Terray, E. A., M. A. Donelan, Y. C. Agrawal, W. M. Drennan, K. K. Kahma, A. J. Williams, P. A. Hwang, and S. A. Kitaigorodskii (1996), Estimates of kinetic energy dissipation under breaking waves, *J. Phys. Oceanogr.*, *26*, 792-807.
- Valenzuela, G. R (1978), Theories for the interaction of electromagnetic and oceanic waves – A review, *Bound.-Layer Meteorol.*, *13*, 61-85.
- Yueh, S. H., B. W. Stiles, W.-Y. Tsai, H. Hu, and W. T. Liu (2001), QuikSCAT geophysical model function for tropical cyclones and application to Hurricane Floyd, *IEEE Trans. Geos. Rem. Sens.*, *39*, 2601-2612.